ELSEVIER

Journal of Structural Geology 26 (2004) 659–677

JOURNAL OF STRUCTURAL GEOLOGY

www.elsevier.com/locate/jsg

The main Variscan deformation event in the Pyrenees: new data from the structural study of the Bielsa granite

T. Román-Berdiel[a,*], A.M. Casas[a], B. Oliva-Urcia[a], E.L. Pueyo[b], C. Rillo[c]

[a]*Departamento de Ciencias de la Tierra. Universidad de Zaragoza, 50009 Zaragoza, Spain*
[b]*Inst. of Geophysics. University of Leoben. Gams 45, A-8130, Frohnleiten, Austria*
[c]*Inst. de Ciencia de Materiales de Aragón. CSIC-Univ. de Zaragoza, 50009 Zaragoza, Spain*

Received 23 January 2003; received in revised form 11 August 2003; accepted 11 September 2003

Abstract

A structural and magnetic fabric study of the Bielsa granite (Axial Zone of the Pyrenees) provides new data indicating that this pluton was emplaced during the main Variscan event recognized in the Pyrenees. We argue that the later post-Triassic deformation was localized along mylonitic bands reactivating earlier Variscan shear bands. The Bielsa granite intrudes Cambro–Ordovician metasediments at its northern border, and the pluton is unconformably overlain by sediments Triassic in age to the south and east. The main structures in the igneous body are magmatic foliations and lineations defined by feldspar phenocrysts and biotite and dextral shear bands with dominant WNW–ESE trends. The WNW–ESE striking magmatic foliations have variable dips, and the magmatic lineation a subhorizontal WNW–ESE trend. The zonation of low-field magnetic susceptibility, coarsely related to mineral content, indicates a layer arrangement of rock-types, with more basic compositions at the northern border. The magnetic ellipsoids are prolate along a WNW–ESE central band, and oblate at the pluton borders, where flattening is more important. All these data allow us to interpret the Bielsa intrusion as being caused by coeval NNE shortening and dextral shear. The presence of shear bands indicates that strain localization under dextral transpression continued during late-Variscan times.

Keywords: Pyrenees; Variscan; Granite; Bielsa; Microstructure; Anisotropy of magnetic susceptibility

1. Introduction

The study of the Variscan structure of the Pyrenees faces the difficulty that two orogenic cycles are superimposed. The Alpine thrusting and folding are responsible for the presently observed overall structure of the range (Déramond et al., 1985; Williams, 1985), and within the Palaeozoic basement it is difficult to ascertain whether the observed thrusts are reactivated Variscan detachments or newly-formed Alpine structures.

Granite bodies can be very useful as kinematic markers, in recording events that are strictly related to their emplacement, through their magmatic foliation and lineation patterns. Progressive deformation during crystallization is well recorded by C–S structures, and by microstructural signatures of high- and subsequent low-temperature solid-state deformation. When deformed in the solid-state, well-defined criteria of shear sense can be derived. However, these structural records correspond to a short time interval when compared with the whole tectonic history of the orogenic belt. And since granites are very hard to pervasively-imprint after their final crystallization, most frequently, in this case they are imprinted only by brittle deformation (joints and faults). Therefore, structural studies within and around granite massifs allow the constraint of the deformational stages in orogens.

In spite of the local overprints of the Variscan structures by the Alpine ones, several structural studies on Variscan granite plutons of the Pyrenees have demonstrated that the main Variscan tectonic phase, called D2 (Zwart, 1986), was transpressional (Leblanc et al., 1996; Evans et al., 1998; Gleizes et al., 1998a,b, 2001). Among these plutons, the Bielsa granite has not been studied until now from the structural point of view. In order to characterise both the Variscan structures in the Bielsa granite and the relative importance of later Alpine deformation, a detailed structural

* Corresponding author. Fax: +34-976-761-106.
E-mail address: mtdjrb@posta.unizar.es (T. Román-Berdiel).

0191-8141/$ - see front matter © 2003 Elsevier Ltd. All rights reserved.
doi:10.1016/j.jsg.2003.09.001

study was carried out. The interest of this study lies in: (1) the location of the Bielsa granite near the southern border of the Axial Zone, allowing complete characterization of the Variscan deformation in this area, south of the large shear band affecting other Pyrenean granites (Gleizes et al., 1997); (2) the elevation differences between the studied sites (more than 1500 m) that allows to check the consistency of the structural study at different structural levels, in both the inner and outer parts of the pluton; and (3) owing to the outcrop conditions, the Bielsa granite helps in constraining the age and geometrical relationships of shear bands distributed throughout the Pyrenees (Soula et al., 1986c). Finally, this study of the Bielsa pluton allows the testing of the transpressional model proposed by Gleizes et al. (1998a).

This study focuses on the structure of the Variscan Bielsa granite that is located in the Axial Zone of the Central Pyrenees (Fig. 1). We intend to establish the relative contribution of the Variscan regional deformation processes to the intrusion of the Bielsa granite. We used field and microstructural data as well as the anisotropy of magnetic susceptibility (AMS) to characterise its internal structure and we relate it to the structural evolution of the wall rocks. AMS reliability was supported by a rock-magnetic study.

2. Geological setting

The Axial Zone of the Pyrenees belongs to the European Variscan Orogen (Fig. 1). The main phase of the Variscan orogeny in the Pyrenees is characterised by a crustal shortening event marked by large-scale south-verging thrusting and subsequent widespread regional penetrative deformation (Soula et al., 1986a), the so-called D2 phase. The U–Pb ages published in the last decade for the Pyrenean granites indicate that the Hercynian plutonism of the Pyrenees is essentially Carboniferous in age, and syntectonic (Romer and Soler, 1995; Paquette et al., 1997; Roberts et al., 2000). The Bielsa granite constitutes a part of the 'Gavarnie–Héas–Barroude–plan de Larri–Bielsa' WNW–ESE elongated structural–metamorphic dome (Mirouse and Barrère, 1993). This dome constitutes the relative autochthonous of the Tertiary Gavarnie thrust (Séguret, 1972). The Bielsa granite forms the largest part of the Bielsa thrust sheet, a south-verging unit located between the Gavarnie and Millares thrust sheets on its top, and the Guarga thrust sheet at its base (Martínez-Peña and Casas-Sainz, 2003). These four nappes define a piggyback-sequenced imbricate thrust system developed during the Tertiary Pyrenean compression. This compressional deformation is also responsible for large- and short-wavelength folding and steeply dipping faulting of the Triassic sedimentary cover of the Bielsa pluton (Fig. 2b). In the southwestern half of the present day outcrop of the pluton, the envelope of folds involving the Triassic units shows an averaged 40° southward dip, whereas in the northeastern half of the pluton this envelope is more or less horizontal (Fig. 2b and c).

The Bielsa pluton is a NW–SE elongated body, with dimensions of 20 × 5 km. Its outcrop area covers about 50 km^2 (Fig. 2a). To the south and east of the pluton, non-metamorphic, post-emplacement Triassic rocks lie unconformably on the igneous and metamorphic Palaeozoic rocks. This cover precludes observation of the southeastern part of the massif, but isolated outcrops are found.

The Bielsa massif displays a compositional zoning

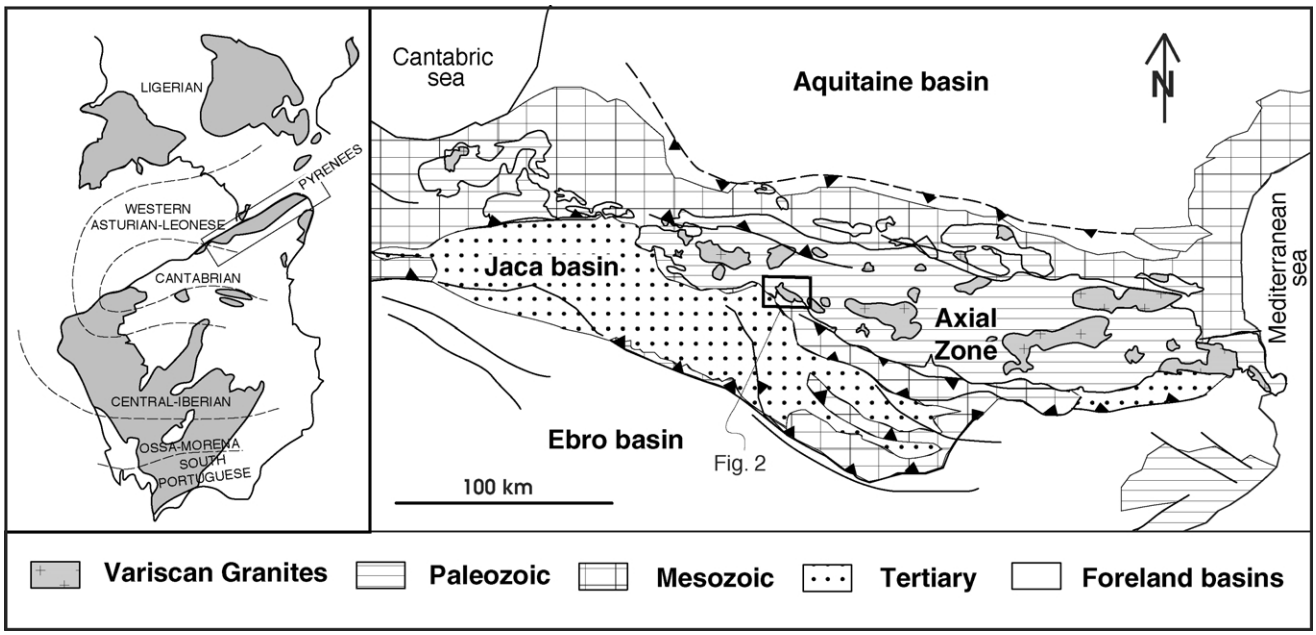

Fig. 1. Geological sketch map of the Pyrenees, showing the situation of the Bielsa granite pluton, and its location in the context of the southern part of the Variscan Europe.

(Enrique, 1989) changing from granodiorite and monzogranite in the south, to tonalite and gabbrodiorite at its northern border (Fig. 2a). Its mineralogical composition mainly consists of quartz, K-feldspar, plagioclase, biotite and hornblende. The texture varies from coarse-grained to porphyritic in a medium-grained matrix. The Bielsa massif is intrusive into metaquartzites and schists of Cambro–Ordovician age, which crop out at its northern border. The northern contact with the country rocks is progressive, with granitic dikes merging in the micaschists and granitic sheets parallel to the main foliation. The intensity of regional metamorphism within the country rocks increases from the northeast to the southwest, reaching the sillimanite isograd near the northern border of the granite and giving migmatites in the Gavarnie and La Larri tectonic windows (Mirouse and Barrère, 1993; Soula et al., 1986b). The Bielsa massif developed a metamorphic aureole in the country rocks, represented by andalousite-bearing hornfels.

3. Field and microstructural data

From a structural point of view, the Bielsa granite is rather heterogeneous, although in many outcrops no mineral preferred orientation can be observed with the naked eye. In some areas, the main deformational structures are a magmatic foliation and lineation, defined by the preferred orientation of feldspar phenocrysts and biotite crystals (Fig. 3a). In other areas, solid-state deformation structures, S–C structures and shear bands (Fig. 4), with biotite concentrated on C planes and a strong stretching lineation on them, can be observed. Moreover, the whole of the massif is pervasively affected at the outcrop scale by brittle faults of probable Tertiary compressional origin. A number of 68 thin-sections were studied in order to characterise microstructures and rock-types.

3.1. Preferred orientation of minerals

They can be observed in a few outcrops (feldspar and biotites; Fig. 3a) and under the microscope (biotites and elongated quartz crystals; Fig. 3c). Other structural markers are mafic enclaves, common in the northeast of the massif, elongated parallel to the preferred orientation of feldspar phenocrysts and also parallel to both the contact with the country rocks (Fig. 3b) and the regional foliation whose regional strike is WNW–ESE (Fig. 2). Along the northeastern border, a preferred orientation of minerals is particularly well defined but kinematic criteria are lacking. This points to a dominantly flattening regime during setting of the granite, although, a clearly defined dextral sense of shear is evidenced in the country rocks (Fig. 3e).

In the granite, quartz grains exhibiting elongated shape and undulose extinction attest to high-temperature straining in the solid state (Fig. 3d). In the country rocks, the chiastolite crystals observed in the slates of the southeastern border (Fig. 3f) are likely coeval with the intrusion of the Bielsa granite. However, it must be taken into account that the pluton has intruded a series affected by a regional metamorphism for which the andalousite isograd is located at the top of the pluton in some areas (Mirouse and Barrère, 1993). Hence the chiastolites may have predated the intrusion of the Bielsa granite.

3.2. Shear bands

Shear bands are observed along the whole outcrop area of the massif (Fig. 4). They are elongated zones, several kilometres long, 100 m thick on average, and show moderate to steeply dipping foliation surfaces. Strikes of these shear bands vary from N060°E to N140°E, but N110°E is the dominant strike (Fig. 4) with a northward dip. The southwestern contact of the granite with the Triassic, dipping to the south, shows a shear band parallel to this contact, strongly altered due to weathering previous to deposition of the Triassic beds. This shear band is, therefore, Variscan in age. Onto the C-planes of these shear bands, strongly imprinted stretching lineations can be observed with highly variable pitches between 0° (pure strike-slip) and nearly 90° (pure reverse). Integrating this variability, the shear bands indicate, however, a dominant dextral shear (Fig. 5), and conjugate sets of sinistral C-planes may be observed in some of the bands. Both, the variable trends of the stretching lineations and the occurrence of conjugate C-planes indicate a contribution of flattening (pure shear) in the bulk deformation associated with these shear bands.

Some of the shear bands contain deformed fragments of the Triassic red sandstones or shales that overlie the granite in the eastern sector (Fig. 5a). This demonstrates the post-Triassic age of either the formation of these shear zones, or at least the reactivation of Variscan shear zones. These shear zones, where pervasive sericitization of feldspars and transformation of biotite into chlorite (Fig. 5d) are present, are sometimes characterized by rocks consisting of quartz porphyroclasts floating in a fine-grained matrix, the whole being cross-cut by C planes (Fig. 5b–d). The quartz porphyroclasts themselves are brittlely deformed, with tension fractures perpendicular to the shear band and numerous fractures with R (15°) to T (45°)-like arrangements, synthetic with the movement of the shear band. All these features definitely point to low-temperature deformation at the brittle–ductile transition (Evans, 1988) during a post-emplacement stage.

4. AMS analysis

Samples for this study were collected from 60 stations distributed throughout the Bielsa granite (Table 1, Fig. 2), with a total of 409 standard specimens analysed. During sampling, the structural complexity resulting from post-emplacement folding involving the Triassic units was taken

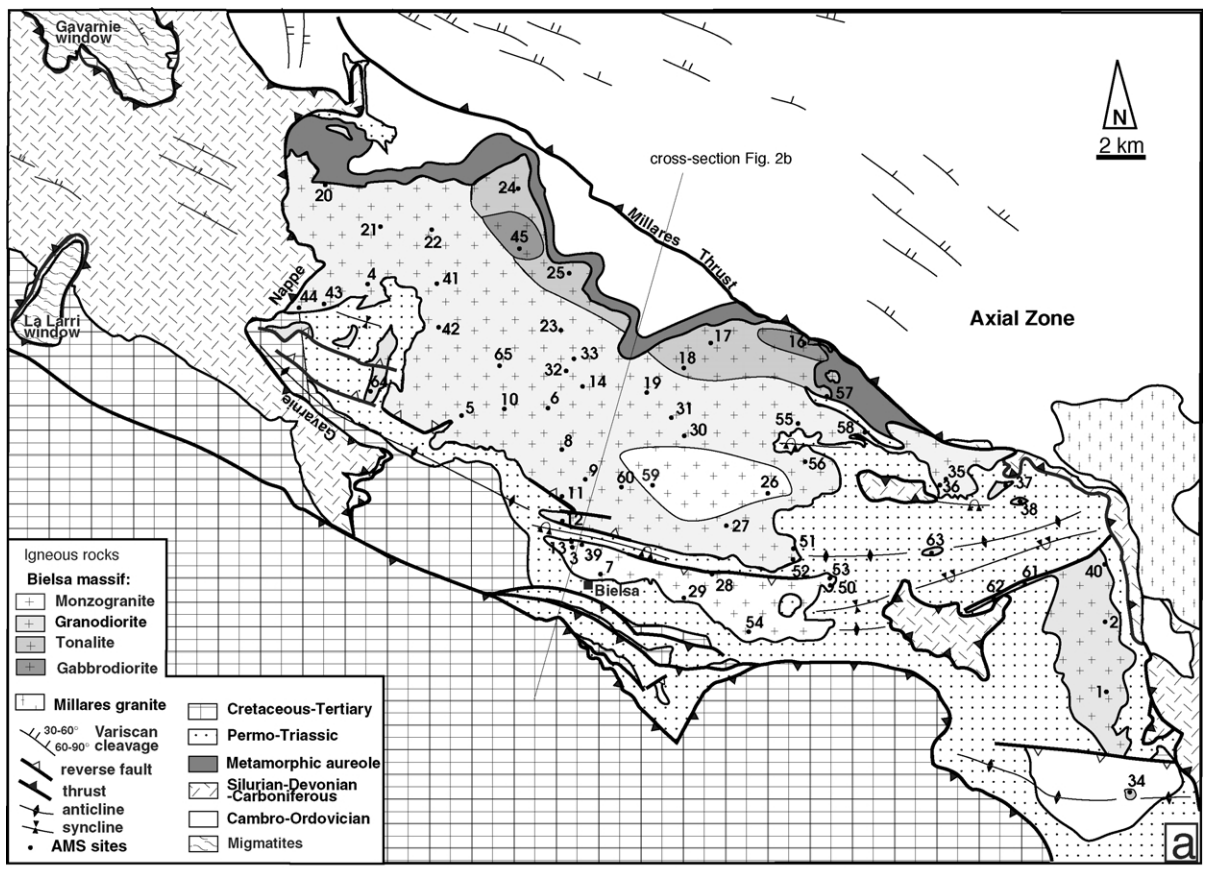
Gavarnie window
La Larri window
Nappe
Gavarnie
Millares Thrust
cross-section Fig. 2b
N
2 km
Axial Zone
Bielsa
Igneous rocks
Bielsa massif:
Monzogranite
Granodiorite
Tonalite
Gabbrodiorite
Millares granite
30-60° 60-90° Variscan cleavage
reverse fault
thrust
anticline
syncline
AMS sites
Cretaceous-Tertiary
Permo-Triassic
Metamorphic aureole
Silurian-Devonian -Carboniferous
Cambro-Ordovician
Migmatites
a

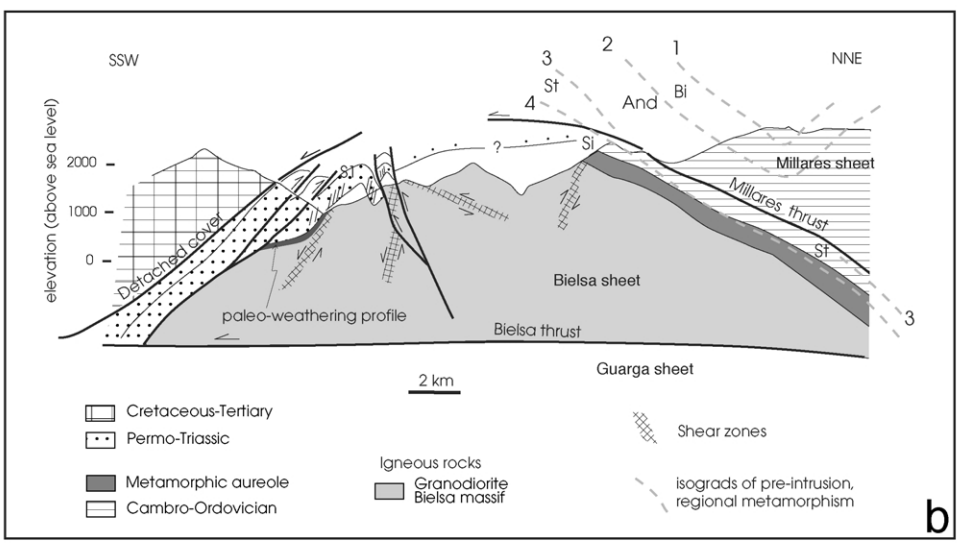
SSW
NNE
elevation (above sea level)
2000
1000
0
Detached cover
paleo-weathering profile
Bielsa thrust
Bielsa sheet
Millares sheet
Millares thrust
Guarga sheet
St
And
Bi
Si
2 km
Cretaceous-Tertiary
Permo-Triassic
Metamorphic aureole
Cambro-Ordovician
Igneous rocks
Granodiorite
Bielsa massif
Shear zones
isograds of pre-intrusion, regional metamorphism
b

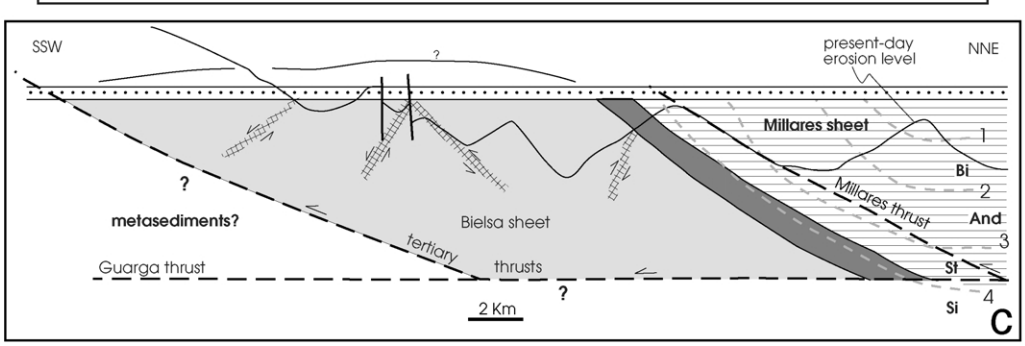
SSW
NNE
present-day erosion level
Millares sheet
Millares thrust
Bielsa sheet
metasediments?
tertiary thrusts
Guarga thrust
2 Km
Bi
And
St
Si
c

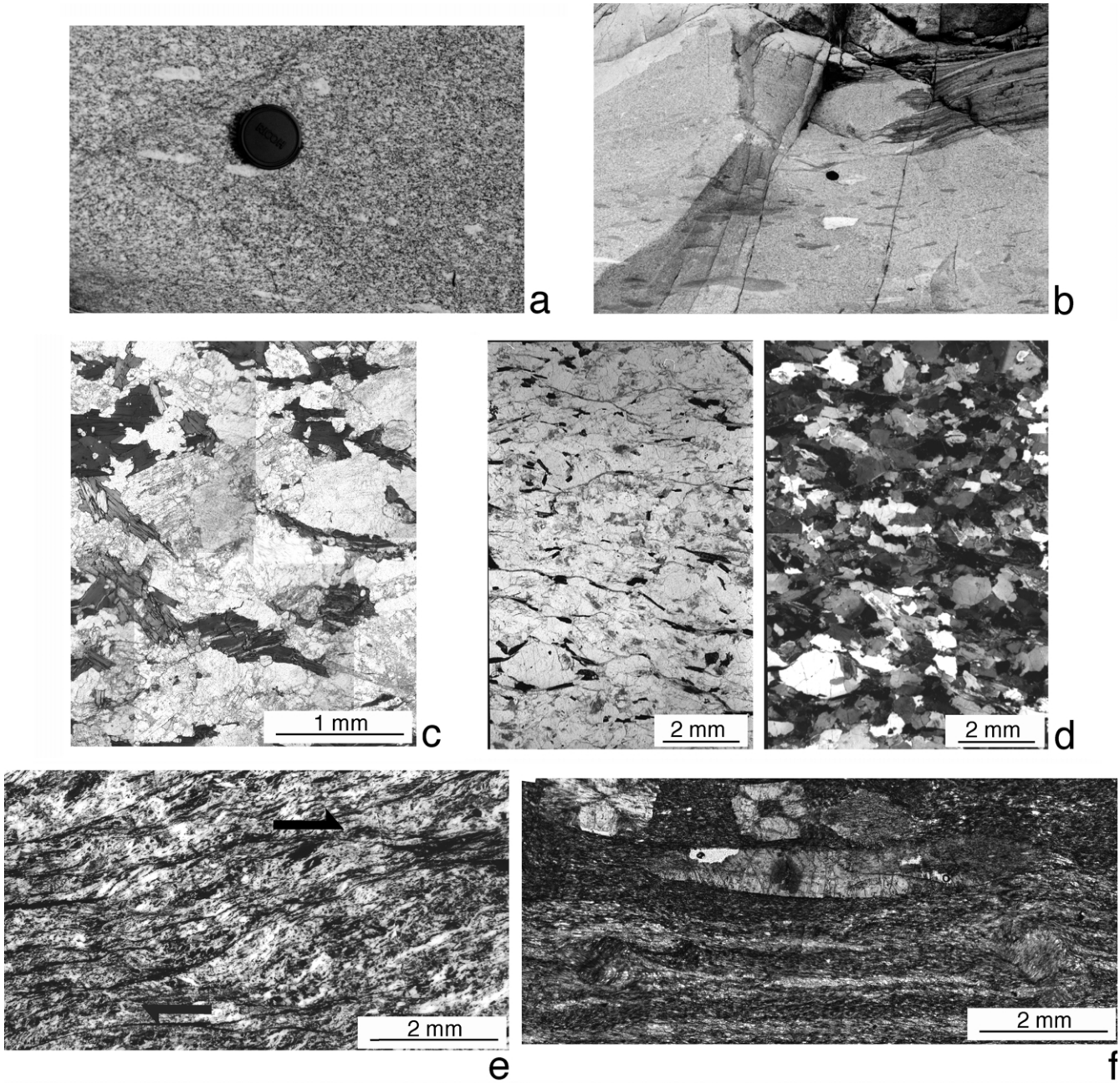

Fig. 3. (a) and (b) Field aspect of preferred orientation of feldspar and biotites, and of elongated mafic enclaves (site 45). (c) Thin section showing preferred orientation of biotites in parallel nicols (site 45). (d) Thin section showing preferred orientation of biotites and elongated quartz grains exhibiting ondulatory extinction, in parallel and crossed nicols (site 24). (e) Mylonitic dextral shear band in the host rocks of the northern border (north to site 24; crossed nicols). (f) Crystals of chiastolite in the slates cropping out at the southeastern border (close to site 34; parallel nicols).

into account. Sampling sites were located next to the two limbs of folds to determine as much as possible the effect of rotation of granite blocks around horizontal axes. In order to prevent the occurrence of complex post-magmatic fabrics, most of the sites are located outside the shear bands. Hence, in places where shear bands are mapped in Fig. 4, note that the cores were drilled outside the shear bands.

At each site, an average of six to seven cores were

Fig. 2. (a) Geological sketch map of the area around the Bielsa massif (simplified and modified from Mirouse and Barrère (1993) and Ríos-Aragüés et al. (1982)), showing the main rock types in the pluton (from Enrique, 1989), and with location of measurement sites. (b) Geological cross-section (see Fig. 2a for location) of the Bielsa thrust sheet. (c) Reconstructed cross-section showing the geometry of the granitic body previous to the Tertiary compressional deformation.

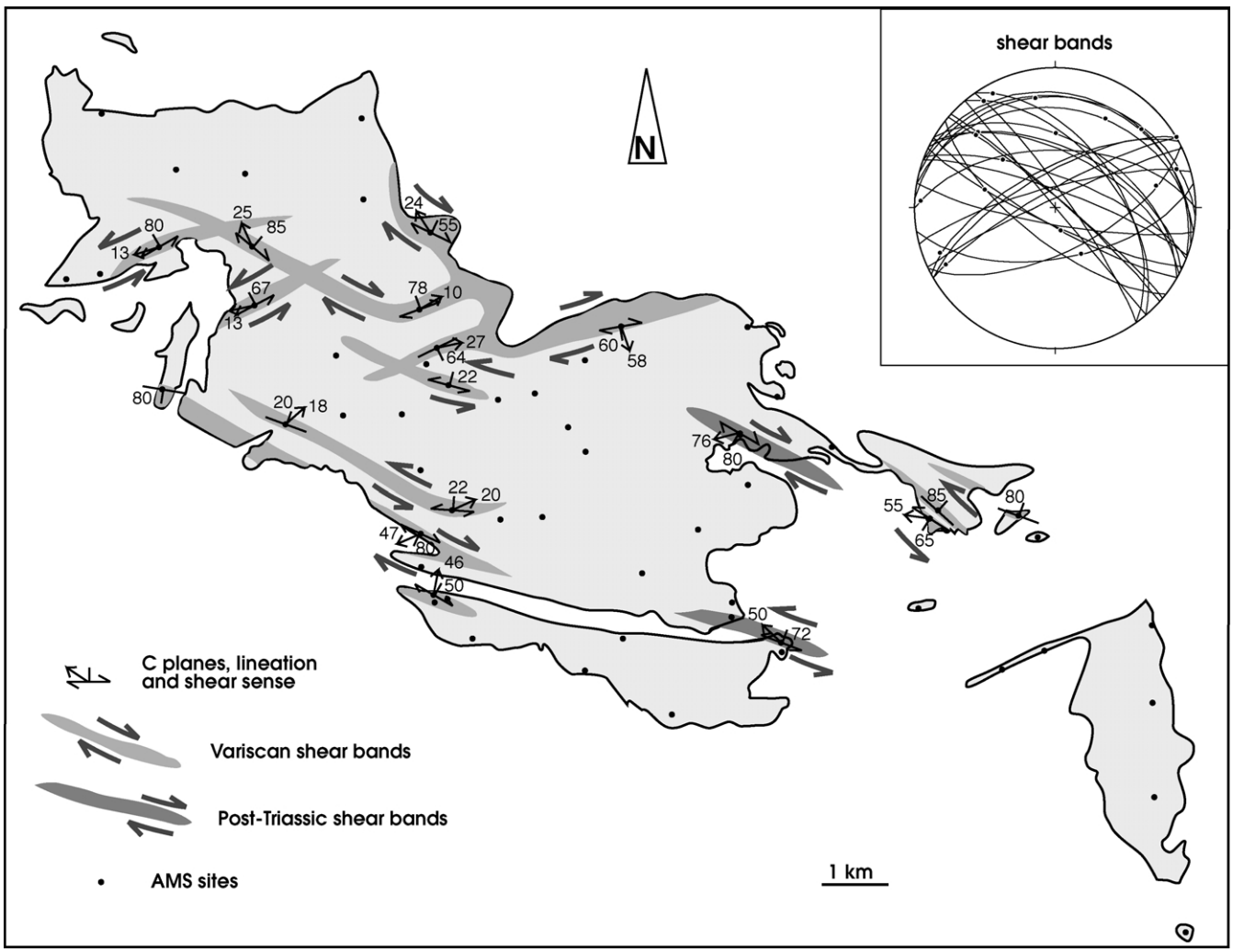

Fig. 4. Field data from shear bands, and Schmidt diagram of C planes and associated stretching lineations.

collected. Measurements were made at room temperature with the KLY-2 susceptibility meter (4×10^{-4} T; 920 Hz) of the University of the Pais Vasco (Bilbao). AMS measurements give the orientations and magnitudes of the $K_{min} \leq K_{int} \leq K_{max}$ axes of the AMS ellipsoid. The magnetic fabric is characterised by the magnetic lineation (K_{max}) and the magnetic foliation (perpendicular to K_{min}). The relationship between tensor axes, normalised by means of Jelinek's method (Jelinek, 1977) (Table 1) was studied using: (i) the corrected anisotropy degree, P' showing the intensity of the preferred orientation of minerals, and (ii) the shape parameter, T, varying between $T = -1$ (prolate ellipsoids) and $T = +1$ (oblate ellipsoids). P' and T parameters are defined as (Jelinek, 1981):

$$P' = \exp\sqrt{\left\{2\left[(\mu_1 - \mu_m)^2 + (\mu_2 - \mu_m)^2 + (\mu_3 - \mu_m)^2\right]\right\}}$$

$$T = \frac{(2\mu_2 - \mu_1 - \mu_3)}{(\mu_1 - \mu_3)}$$

where $\mu_1 = \ln K_{max}$, $\mu_2 = \ln K_{int}$, $\mu_3 = \ln K_{min}$ and $\mu_m = (\mu_1 + \mu_2 + \mu_3)/3$.

4.1. Magnetic mineralogy and magnetic susceptibility

Bulk susceptibility (K_m) ranges from 17×10^{-6} SI (site B44) to 822×10^{-6} SI (site B16, Table 1), most parts of the massif having low susceptibilities (Fig. 6), the average bulk susceptibility being 181×10^{-6} SI. Susceptibilities higher than 300×10^{-6} SI are found in seven sites only. Hence, except in those sites where some ferromagnetic contribution likely occurs, a paramagnetic susceptibility dominates carried by the iron-bearing silicates (biotite, amphibole) (Gleizes et al., 1993; Borradaile and Henry, 1997; Bouchez, 1997, among others).

Acquisition curves of isothermal remanent magnetization (IRM) were obtained in four samples covering the whole range of susceptibility. The sample, carrying a saturation IRM at 2.5 T, is exposed to reverse fields of increasing strengths (back field experiments). Then, its remanence decreases to zero at a field called the coercivity of remanence, H_{cr}. A DC-SQUID magnetometer was used together with a pulse magnetizer (2-G instruments) in the Gams paleomagnetic laboratory (Austria). IRM gaining

Table 1
AMS data for 60 sampling stations of the Bielsa pluton. K_1 and K_3, mean (trend/plunge) of the magnetic lineation and of the pole of the magnetic foliation considering a unimodal distribution (Fisher, 1953); α_{95}, opening angle for the confidence cone with the 95% probability; K_m, magnitude of the magnetic susceptibility (in 10^{-6} SI); P', anisotropy degree; T, shape parameter

Site	*Number of samples*	K_1	α_{95}	K_3	α_{95}	K_m	P'	T
1	8	107/35	7	306/53	9	175	1.044	0.220
2	4	071/13	67	304/72	9	155	1.039	0.188
3	4	271/8	15	005/29	11	133	1.031	0.108
4	8	309/15	39	180/65	25	153	1.017	0.077
5	9	112/17	20	220/44	27	208	1.155	0.242
6	7	092/7	34	241/76	20	157	1.027	0.127
7	4	102/14	28	002/33	8	140	1.034	0.239
8	7	308/28	29	185/51	28	137	1.020	0.147
9	5	120/4	45	220/79	41	146	1.015	−0.010
10	4	098/13	43	252/82	48	152	1.023	0.346
11	7	062/64	37	208/15	36	23	1.041	0.003
12	4	091/47	37	246/49	32	133	1.022	0.330
13	5	113/7	11	026/5	30	111	1.027	0.366
14	6	147/20	35	238/18	29	137	1.018	−0.062
16	6	331/63	35	159/50	51	822	1.051	−0.121
17	8	074/36	14	166/3	21	412	1.031	0.073
18	6	126/10	31	248/59	22	476	1.032	0.346
19	8	039/11	15	134/14	17	178	1.022	−0.015
20	4	058/18	21	165/38	16	168	1.055	0.274
21	4	272/18	34	083/65	32	64	1.040	0.381
22	4	272/36	57	141/35	83	23	1.040	0.220
23	7	088/15	39	358/1	22	148	1.047	0.157
24	5	155/18	12	280/60	18	63	1.218	0.675
25	5	121/23	35	194/28	47	496	1.118	0.259
26	5	002/20	42	117/39	51	134	1.016	−0.154
27	5	245/12	43	346/41	32	159	1.017	−0.057
28	4	089/20	37	196/29	38	137	1.033	0.174
29	11	326/12	19	230/2	31	47	1.026	−0.025
30	6	133/78	42	290/10	47	186	1.018	0.089
31	6	231/5	44	308/6	37	161	1.013	0.142
32	4	301/37	25	175/43	50	46	1.033	−0.011
33	7	058/45	12	193/37	10	91	1.046	0.312
34	4	148/6	13	058/48	46	373	1.018	0.190
35	4	359/71	84	316/66	78	188	1.023	0.356
36	7	008/56	27	210/32	11	180	1.044	0.397
37	4	294/17	24	200/21	24	286	1.049	0.277
38	4	061/0	42	121/85	62	134	1.038	0.118
39	8	267/12	16	007/50	12	160	1.027	0.264
40	6	134/28	55	261/80	48	251	1.027	−0.140
41	6	317/19	43	191/51	36	151	1.019	−0.086
42	9	097/7	19	353/64	29	147	1.017	−0.417
43	6	101/23	30	005/33	29	147	1.014	−0.301
44	10	086/12	24	184/54	25	17	1.027	−0.113
45	15	123/31	18	317/65	24	568	1.155	0.113
50	9	211/1	34	336/51	25	130	1.015	0.258
51	9	210/16	28	355/66	22	147	1.025	0.362
52	9	152/56	24	291/32	29	296	1.165	−0.119
53	8	332/50	10	206/25	12	91	1.020	0.248
54	9	062/17	28	331/49	25	126	1.019	0.150
55	9	028/29	28	136/20	32	167	1.033	0.001
56	9	076/26	36	211/51	11	158	1.036	0.427
57	9	304/14	25	158/71	20	327	1.040	0.206
58	6	187/4	16	297/68	18	116	1.096	0.417
59	9	035/28	11	214/63	7	124	1.021	0.202
60	9	028/55	34	240/23	23	115	1.015	0.054
61	8	110/40	30	214/14	11	174	1.020	0.460
62	9	097/18	12	265/70	8	155	1.029	0.326
63	7	024/8	9	118/16	13	105	1.033	−0.248
64	9	063/0	39	194/77	34	128	1.019	0.056
65	8	103/21	14	225/57	26	110	1.017	−0.070

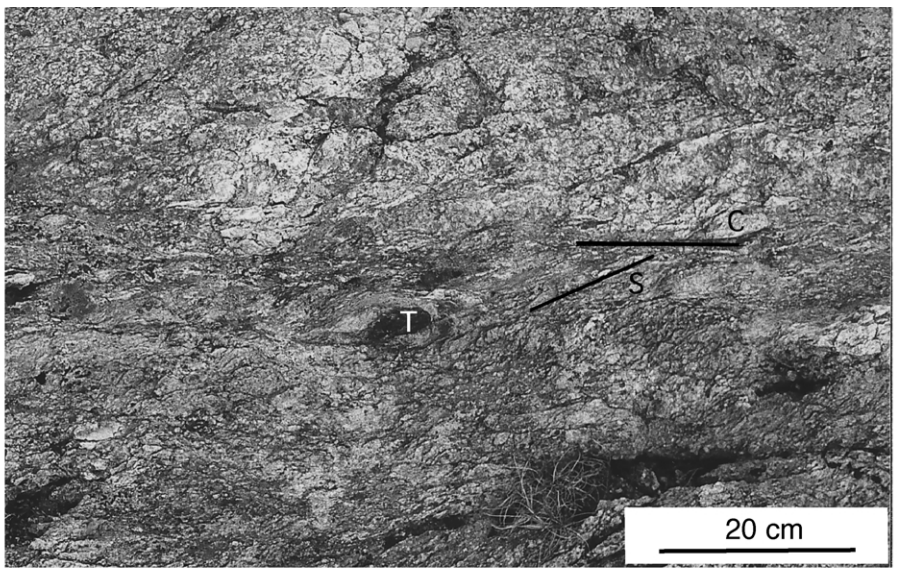

a

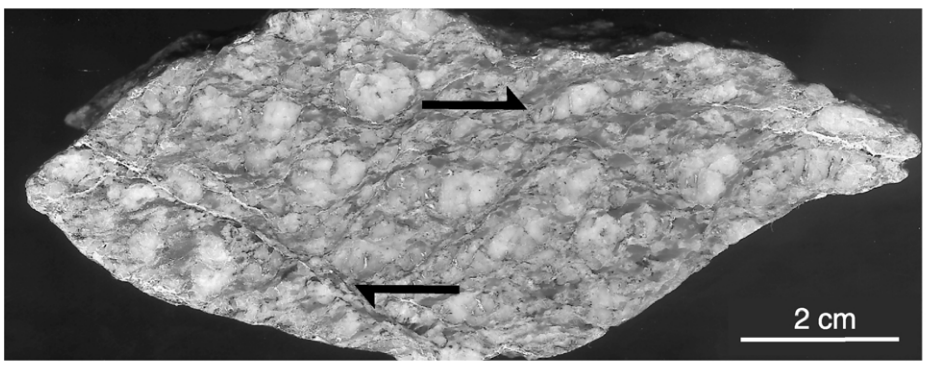

b

c

d

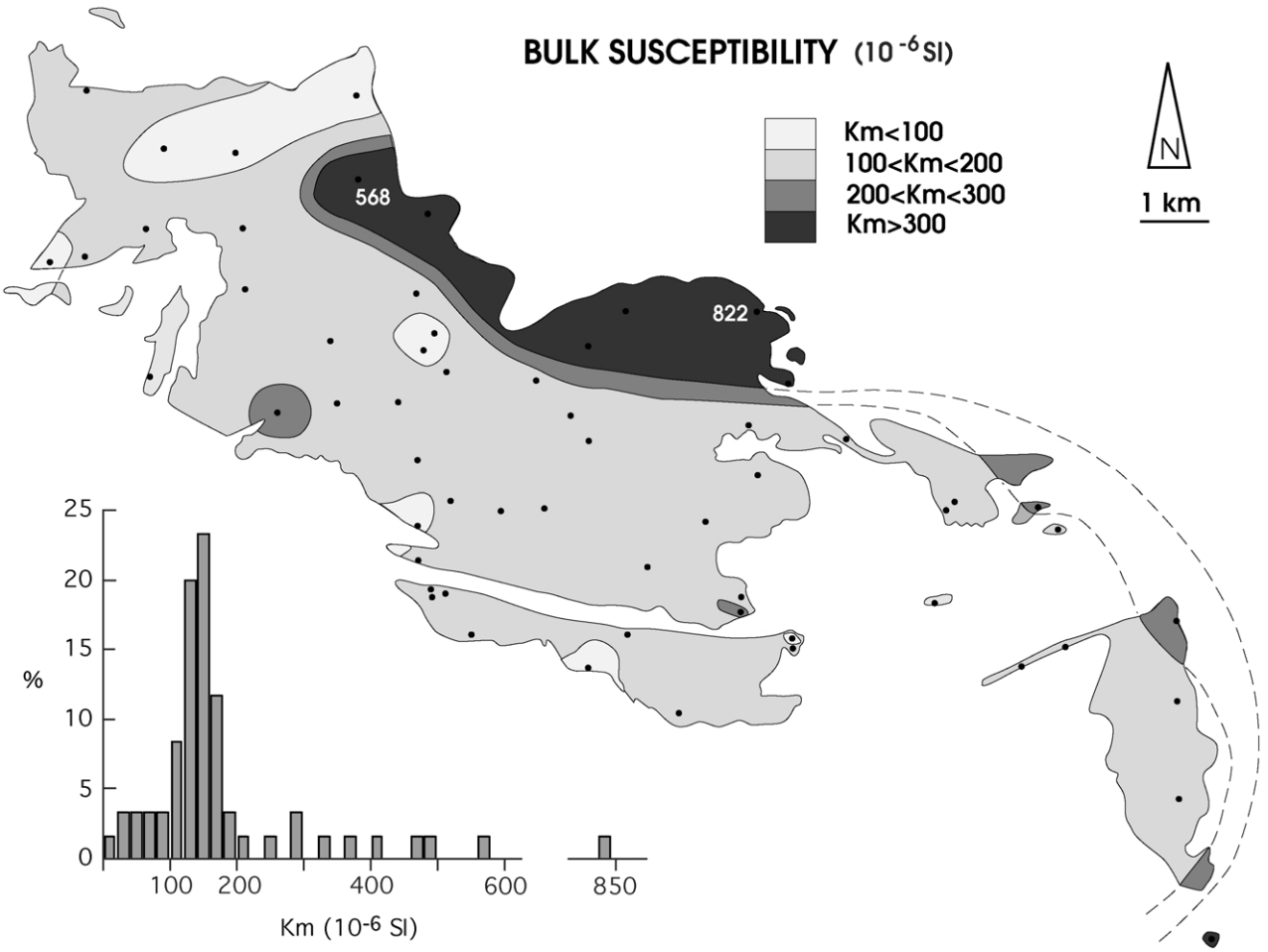

Fig. 6. Bulk susceptibility map (K_m in 10^{-6} SI) and frequency histogram of the Bielsa pluton.

patterns (Fig. 7a) show a quick saturation for relatively small magnetic fields. In all samples, more than 70% of saturation was reached at 0.3 T. Therefore, a widespread occurrence of low coercivity ferromagnetic minerals (s.l.) can be inferred in the Bielsa granite. Back field experiments after saturation showed very low H_{cr} values (between 0.55 and 0.75 mT) (Fig. 7a).

To control unblocking temperatures, thermal demagnetisation of three IRM components were also done, as proposed by Lowrie (1990) using an MMTD oven. To obtain information about high, intermediate and low coercivity carriers, degree of saturation per axes were 1.45, 0.4 and 0.12 T. Unblocking temperatures of B-17 and B-5 samples are about 500°C (Fig. 7b), indicating the occurrence of a low to intermediate coercivity mineral, probably magnetite. Previous reports on ferromagnetic (s.l.) minerals in granitic rocks (Pueyo et al., 1995; Pignotta and Benn, 1999; Beck et al., 2000, among many others) together with the equilibrium reactions of iron-bearing minerals in granites (Frost and Lindsley, 1991) strongly suggest that magnetite is the main carrier of the remanence.

Hysteresis loops at room temperature were performed to constrain the magnetic mineralogy, using the SQUID magnetometer (model MPMS-5S, Quantum Design) at the University of Zaragoza (Spain). From the hysteresis data, the paramagnetic (K_{para}) and ferromagnetic (K_{ferro}) contributions to K_m can be determined (Borradaile and Werner, 1994). The constant slope of the hysteresis curves after saturation (between 0.5 and 1 T; Fig. 8a) represents the pure paramagnetic (K_{para}) contribution to the bulk susceptibility (K_m). The K_{para} component of the susceptibility is dominated by biotite, which is present in all the samples. The hysteresis loops due to the ferromagnetic contribution also indicate the occurrence of very low coercivity minerals in all cases, with complete saturation at 0.3 T (Fig. 8b). If magnetite is assumed to be the main carrier, a multi-domain grain size is prevalent as deduced from the Day et al. (1977)

Fig. 5. (a) Field aspect of a post-Triassic shear band affecting the granite and including fragments of Triassic formation (T) (site 53). (b) Aspect of a shear band in a *XZ*-polished section (site 12). (c) and (d) Different aspects of the shear bands in thin section. (c) Quartz porphyroclasts floating in a fine-grained clayey matrix (crossed nicols; site 9). (d) Alteration of biotite into chlorite and fracturing of chlorite (parallel nicols; site 55).

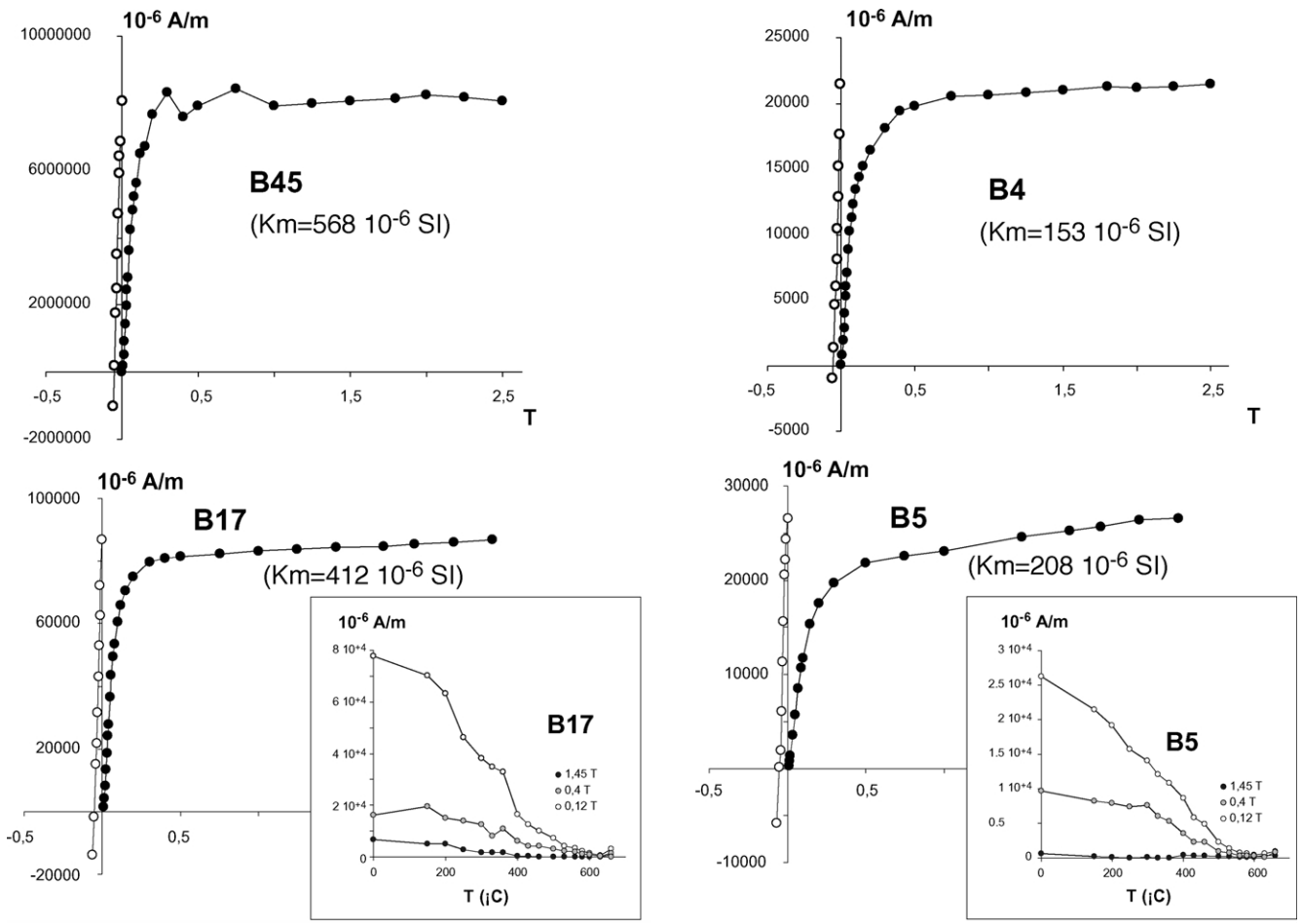

Fig. 7. (a) IRM, back field experiments and (b) thermal demagnetisation of three components IRM (see text for details). The selected samples (Table 1) cover the whole susceptibility range (K_m) found in the pluton, and show characteristic low coercivity acquisition curves.

diagram (Fig. 8c). The ferromagnetic contribution (% K_{ferro}) to the bulk susceptibitity (K_m) is significant in all samples studied, showing low (sites B-45 and B-18 with 12 and 25%, respectively) to intermediate values (sites B-4 and B-9, 33 and 38%, respectively). These results evidence that the Bielsa granite, which could be classified as paramagnetic granite, is actually not paramagnetic, since the presence of magnetite is evidenced by the thermal demagnetisation of three IRM components and the hysteresis loops.

Theoretically, the ferromagnetic contribution prevents the correlation of the bulk susceptibility (K_m) with the iron content and, therefore, with the petrographic type. In spite of this, a good correlation between the independently mapped out lithological zonation (Enrique, 1989) and the susceptibility zonation of the Bielsa massif is observed (compare Figs. 2 and 6). Some differences appear, however, in the northern sector where K_m shows the lowest values. From optical microscopy observations, a smaller content on biotite is indeed verified in this sector. The following correlations can be established between the magnetic susceptibilities and the petrographic types defined by Enrique (1989):

$$K_m > 500 \times 10^{-6}\text{SI} = \text{gabbrodiorite}$$

$$500 \times 10^{-6}\text{SI} > K_m > 300 \times 10^{-6}\text{SI} = \text{tonalite}$$

$$300 \times 10^{-6}\text{SI} > K_m > 100 \times 10^{-6}\text{SI} = \text{granodiorite and monzogranite}$$

$$K_m < 100 \times 10^{-6}\text{SI} = \text{leucogranite}$$

Similar good correlation between magnetic susceptibilities and petrographic types have also been observed in other Pyrenean granites (Leblanc et al., 1994; Gleizes et al., 1993, 1998b, 2001), many of them showing a concentric

compositional zonation. In the Bielsa granite, the complete mapping of the facies pattern is hampered in the southeast by the Triassic cover. However, the existence of a tonalitic zone only in the northernmost part of the pluton points to a sheeted arrangement of rock-types, similar to the Trois–Seigneurs granite body (Leblanc et al., 1996), with two dominant lithologies. The K_m zoning (Fig. 6) shows maxima along most of the northern border of the pluton. The lowest values appear in the northwest, where biotite is also less abundant. The central and southern parts of the massif show intermediate values.

Although magnetite is prevalent in multi-domain grain size in the Bielsa granite, site 45 shows traces of single-domain. Image analysis was carried out in order to test that the AMS ellipsoids for the magnetic fabrics correspond to the shape preferred orientations of the biotite crystals. For site 45 three thin sections were prepared that were oriented perpendicular to the principal directions of the AMS. The shape preferred orientations (SPO) of biotite in each image were measured using the INTERCPT program (Launeau and Robin, 1996; Launeau and Cruden, 1998). Image analysis results (Fig. 9) confirm that the AMS closely approximates the biotite-preferred orientations even in this case.

Moreover, in magnetite-bearing granites, it has been indeed demonstrated that the magnetic fabric of magnetite is similar to the magnetic fabric of biotite (Grégoire et al., 1998). Therefore, with a good first order approximation, the AMS directional measurements do provide the preferential orientation of the biotites (Rochette, 1987; Jover et al., 1989; Launeau, 1990; Darrozes et al., 1994). This hypothesis is reinforced by the absence of correlation between the degree of anisotropy, the shape of the AMS ellipsoid and the bulk susceptibility (Fig. 10a and b). This probably indicates that the P' and T values are dominantly influenced by the variations in the preferred orientation of biotite crystals, and that the ferromagnetic crystals display fabrics that are poorly anisotropic. The degree of anisotropy and the shape of the AMS ellipsoid (Fig. 10c) can then be confidently interpreted as a structural indicator in the Bielsa granite.

4.2. Magnetic fabric

The dominant strike of the magnetic foliation is WNW–ESE, with variable dips, northward dips dominating in the northern half of the massif (Fig. 11a). In the orientation diagram (Fig. 11a; whole pluton), the poles of magnetic foliations are distributed on a great circle whose pole plunges 12° to the ESE. Along the southern side of the pluton, post-Triassic folds seem to have played a role in the orientation distribution of foliation planes since strong changes in dips, up to opposite senses, are recorded in the two limbs of Alpine E–W folds. These variations in dips are particularly spectacular when comparing the magnetic foliation measurements of Fig. 10 corresponding to the 12–13 and 50–53 pairs of sites (Fig. 2a). In other sites of the pluton, only small variations in dip are found (sites 55–56), in spite of strong dip variations of the folded cover. Where the Triassic unconformity is horizontal (central–northern part) dip variation of the magnetic foliation is also recorded (Fig. 11a; northern sector) within a dominant northward dip. In the southern sector, where the Triassic unconformity dominantly dips to the south, the magmatic foliation is mostly subhorizontal (Fig. 11a; southern sector).

Note that a bulk tectonic correction applied to the whole southern sector, according to the dominant tilt of the Triassic unconformity, would result in a dominant orientation of magmatic foliations very similar to that of the northern sector. Conversely, note that without this tectonic correction, it is common in many granites that poles of foliations distribute in great circles, even without post-emplacement folding (Aranguren et al., 1996).

Several foliations, mostly located in the central and eastern parts of the pluton, strike N–S to ENE–WSW, instead of WNW–ESE. Some of them are steeply dipping and carry lineations trending N–S to ENE–WSW, although some of them are steeply plunging. This central part of the pluton, where roughly concentric distributions are recorded, could be viewed as a root-zone for the pluton.

Magnetic lineations show a majority of WNW–ESE trends, parallel to the elongation of the pluton in map view, and they mostly plunge to the SE (average: 18/098; Fig. 11b). Since this average trend is more or less parallel to the axis of the post-Triassic compressional folds, the lineations are not expected to be substantially deflected by these folds. Deflections from the mean lineation orientation, however, are mainly located in the central and northeast areas of the massif, roughly coinciding with the area where foliation deviates from its major direction (Fig. 11a).

4.3. AMS scalar data

The degree of magnetic anisotropy P' is rather low in 90% of the specimens, between 1.015 and 1.055 (Table 1, Fig. 10a and c). Such low values are currently recorded in granites having magmatic fabrics and for which the anisotropy is mainly carried by biotite. The iso-contours of P' are elongated in the WNW–ESE direction, and this is consistent with the elongation of the pluton in map view (Fig. 10d). P' is higher than 1.090 in six stations, four of them belonging to the northeastern border, where the granite foliation is strongly defined in the outcrop, and the remaining two stations are found in sites 5 and 52 where a shear band has been mapped (Figs. 2 and 4). In most of the central part of the massif, P' is below 1.020.

The shape parameter, T, of the magnetic ellipsoids (Fig. 10c and e) also varies according to location, prolate ellipsoids being preferentially distributed along a central band parallel to the elongation of the pluton in map view. Oblate ellipsoids dominate along the northern and southern borders of the pluton, suggesting that flattening was more important in these areas. At least for the northern border,

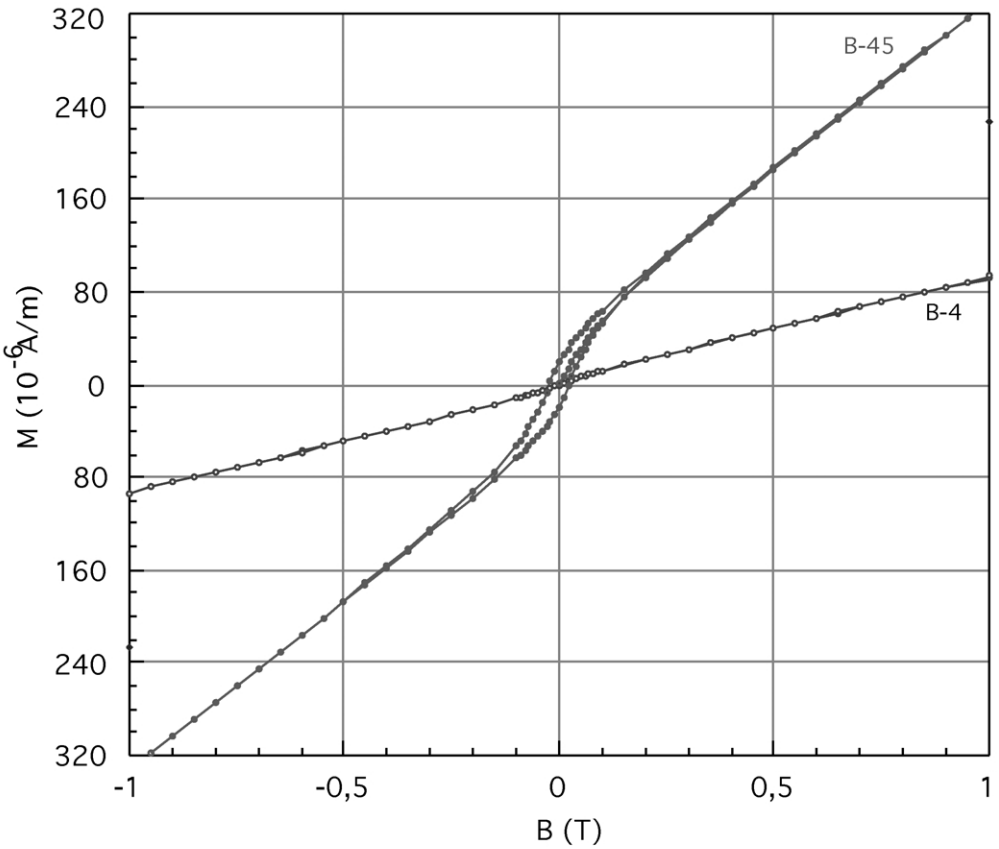
B-45
B-4
M (10-6A/m)
B (T)
320
240
160
80
0
80
160
240
320
-1
-0,5
0
0,5
1

a

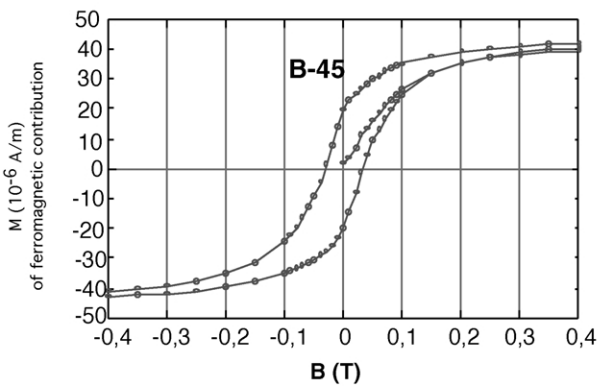
B-45
M (10-6 A/m)
of ferromagnetic contribution
B (T)
50
40
30
20
10
0
-10
-20
-30
-40
-50
-0,4
-0,3
-0,2
-0,1
0
0,1
0,2
0,3
0,4

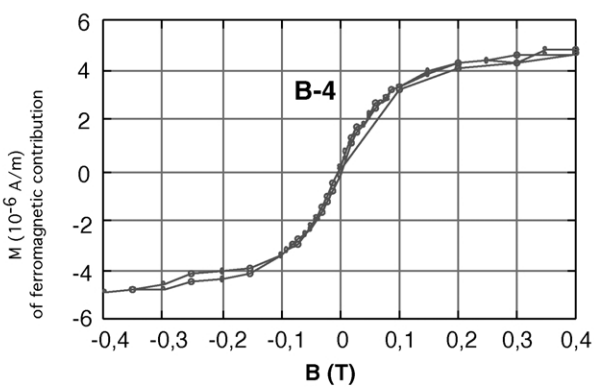
B-4
M (10-6 A/m)
of ferromagnetic contribution
B (T)
6
4
2
0
-2
-4
-6
-0,4
-0,3
-0,2
-0,1
0
0,1
0,2
0,3
0,4

b

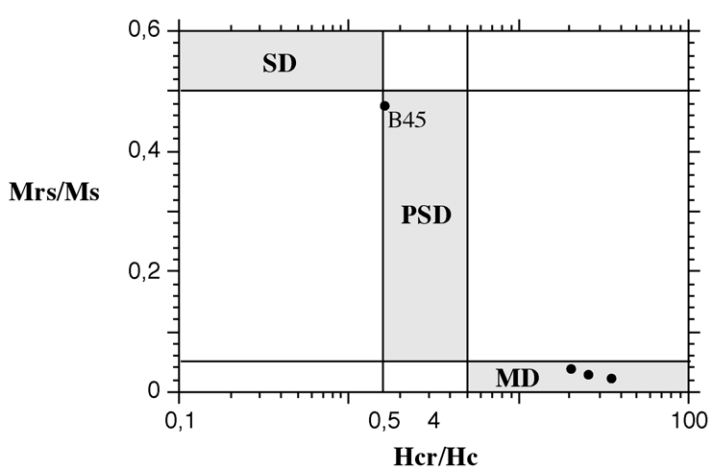
SD
B45
PSD
MD
Mrs/Ms
Hcr/Hc
0,6
0,4
0,2
0
0,1
0,5
4
100

c

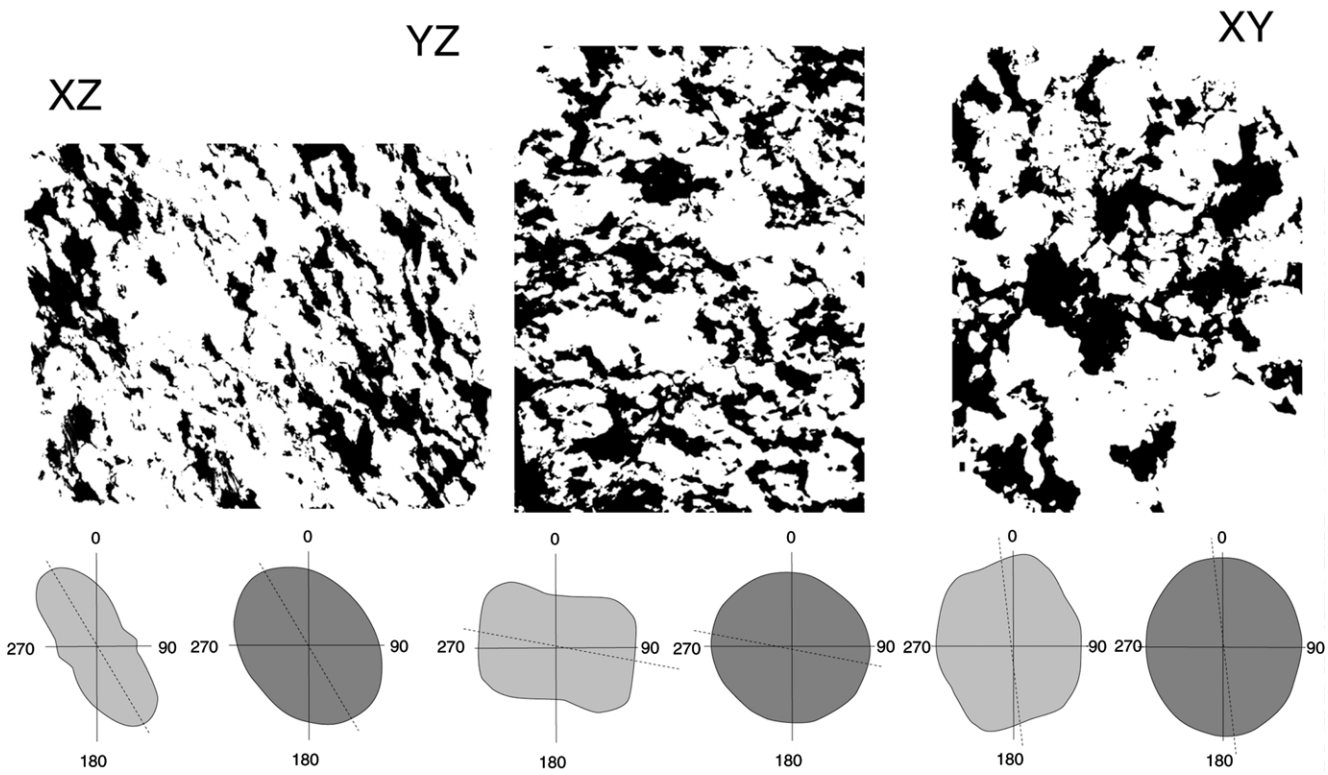

Fig. 9. Results of the image analysis of the biotite preferred orientation in three planes orthogonal to the principal directions of the AMS for tree samples of site 45: black biotite, white quartz and feldspar phases. For each section rose of direction, intercept counts and characteristic shape were calculated from the Fourier series representation of the rose.

which is an intrusive contact, this flattening can be ascribed to pluton emplacement.

From the maps comparing P' and T (Fig. 10d and e), we confidently infer that the pluton underwent a partition of its deformation in relation with its emplacement, into a strong and planar anisotropy along its northern border contrasting with a weak and linear anisotropy along its axis.

5. Interpretation

5.1. Inferred geometry of the Bielsa granite

Constraining the geometry of the pluton is a first step to infer its mode of emplacement. Although gravimetry is usually the key to determine the 3-D shape of igneous bodies, in this case the Bielsa granite is a part of a Tertiary thrust sheet and, according to our macrostructural interpretation (Fig. 2), it is probably cut by a shallow-dipping thrust (Bielsa thrust) belonging to the Axial Zone antiformal stack (Muñoz, 1992; Martínez-Peña and Casas-Sainz, 2003). Therefore, it is not possible to constrain its geometry from gravimetric studies. To reconstruct the geometry of the Bielsa granite body before the Tertiary compression, the only constraint comes from the geometry of the Triassic deposits. The large-scale post-Palaeozoic geometry of the Bielsa thrust sheet can be inferred as an E–W-trending monocline with a subhorizontal sector occupying at present all the central and northeastern parts of the massif (Fig. 2). The south dipping, southern limb of the monocline crops out at the southern outcrop limit of the Bielsa thrust sheet (Fig. 2).

In the reconstruction proposed (Fig. 2c) the Bielsa granite body would have a sheet-like geometry, dipping to the north. This original sheet-like geometry of the Bielsa pluton probably favoured the reactivation of both its northern and southern limits as thrust surfaces during the Tertiary compression. Accordingly, its southern limit formed the frontal ramp of the Bielsa thrust sheet, and its northern limit became parallel to the overlying Millares thrust. The reconstruction of the pre-Triassic, syn-emplacement geometry is even more speculative, since erosion preceding the deposition of the Trias may have eliminated

Fig. 8. (a) Initial hysteresis loops for the four selected samples. (b) Loops with paramagnetic susceptibility subtracted. (c) Hysteresis parameters together with the remanent coercivity deduced from the back field experiment can be used as an approach of the grain size distribution of magnetite (Day et al., 1977). In the Bielsa granite a dominant multi-domain (MD) size is widespread. Only one sample (B45) shows traces of SD (single-domain) magnetite. Hysteresis parameters have been calculated after subtracting the paramagnetic contribution.

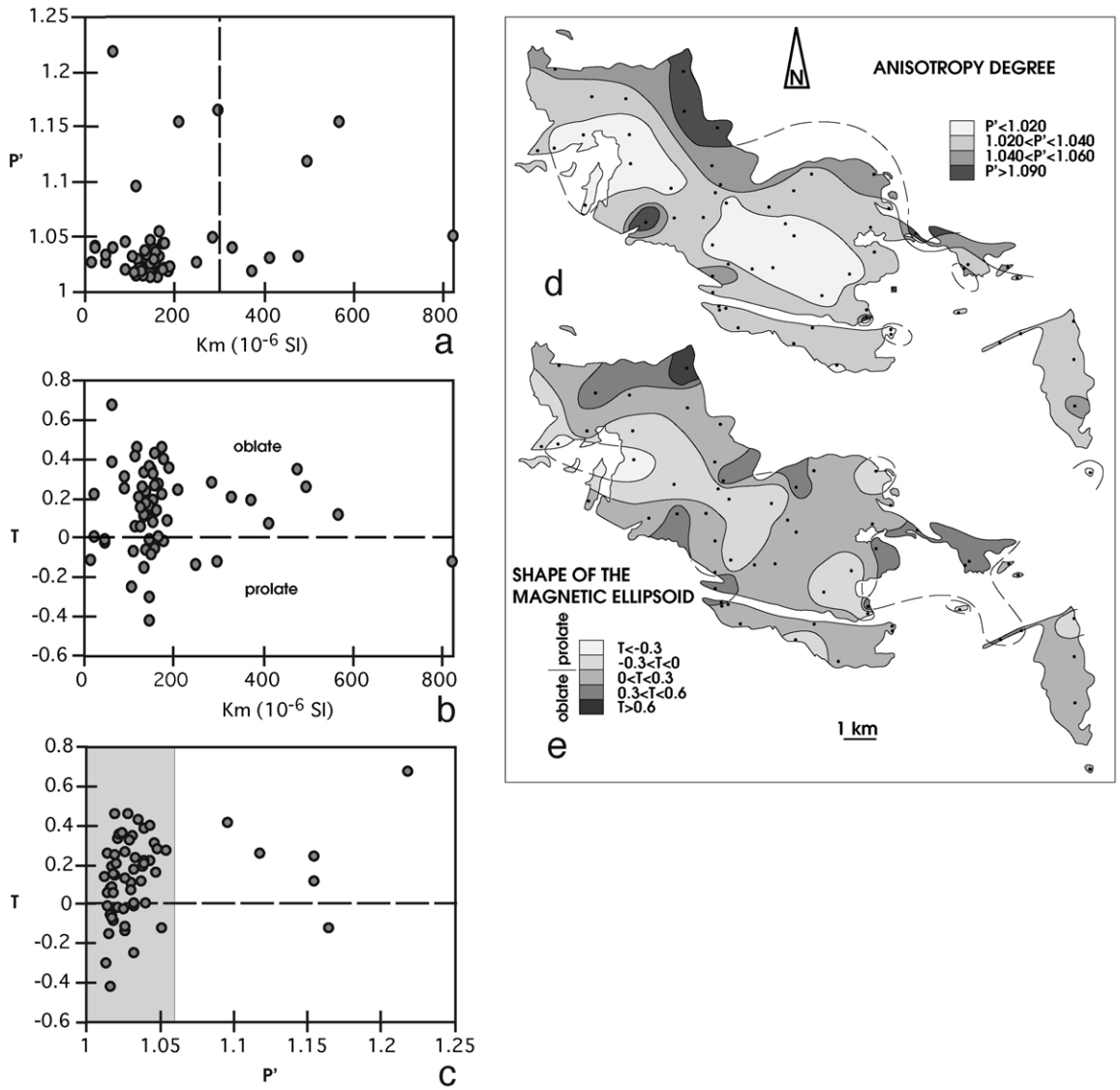

Fig. 10. (a) Anisotropy degree (P') vs. magnetic susceptibility (K_{mean}). The broken line indicates approximately the limit between dominant paramagnetism and dominant ferromagnetism. (b) Shape parameter (T) vs. magnetic susceptibility (K_{mean}). (c) Shape parameter (T) vs. the anisotropy degree (P'). The dashed area corresponds to the typical values for magnetic fabrics. (d) Anisotropy degree (P') map. (e) Shape parameter (T) map.

several kilometres of meta-sedimentary country rock of the granite (Fig. 12). Considering the parallelism between the structures in the granite and the country rock, and the constant northward dip of Variscan structures in this area, an asymmetrical sheet shape with probable flat top can be proposed for the Bielsa granite.

Although it is not possible to corroborate the hypothesis from gravimetric studies, a possible root zone located at the central part of the massif can be inferred from deviations to the dominant strike of the magnetic foliations and lineations (Fig. 11).

5.2. Mode of emplacement

The field structural relationships described above suggest that the Bielsa pluton was emplaced syn-tectonically, during the main compressional stage (D2) in the Variscan Pyrenees, given that the granite emplacement is coeval with a NE–SW flattening direction, perpendicular to the main foliation in the granite and in the country rocks (Fig. 13). Gleizes et al. (1998a) proposed that the main Variscan phase in the Pyrenees is a dextral transpression. From the data obtained in this work it results directly that the emplacement of the Bielsa granite was contemporary with NE–SW (in present-day coordinates) shortening and WNW–ESE stretching, consistent with the attitude of magmatic fabrics (Fig. 13). Moreover, subhorizontal lineations agree with a wrench-dominated transpressional regime (Tikoff and Greene, 1997). However, sigmoidal patterns of foliation, evidence supporting transpressional conditions in other Pyrenean granites (Leblanc et al., 1996; Evans et al., 1998; Gleizes et al., 1998a,b, 2001), cannot be

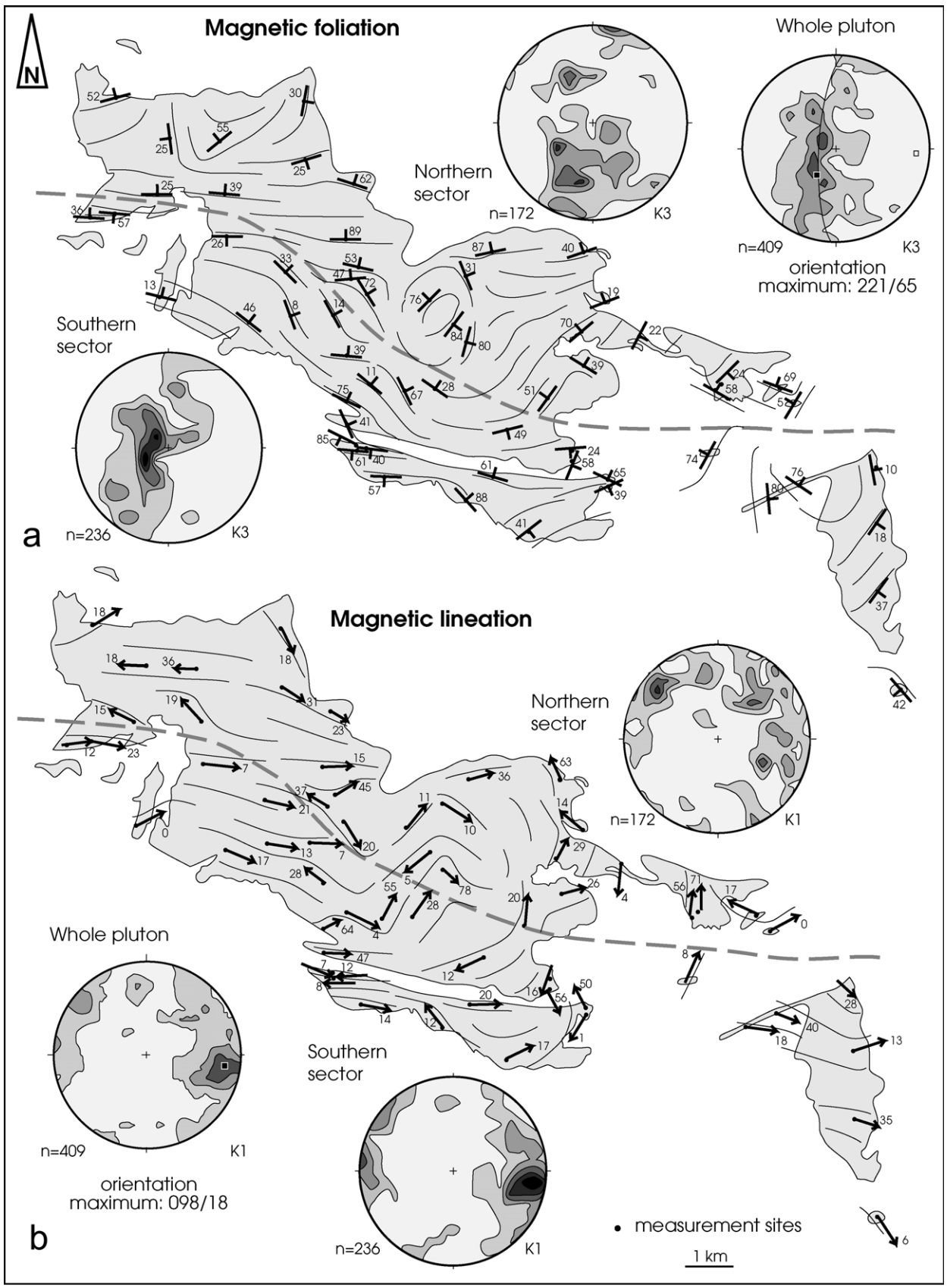

Fig. 11. Structural maps of the Bielsa massif. Magnetic foliations (a) and lineations (b) with simplified trajectories. Density diagrams in Schmidt net, lower hemisphere, contour intervals: 1%.

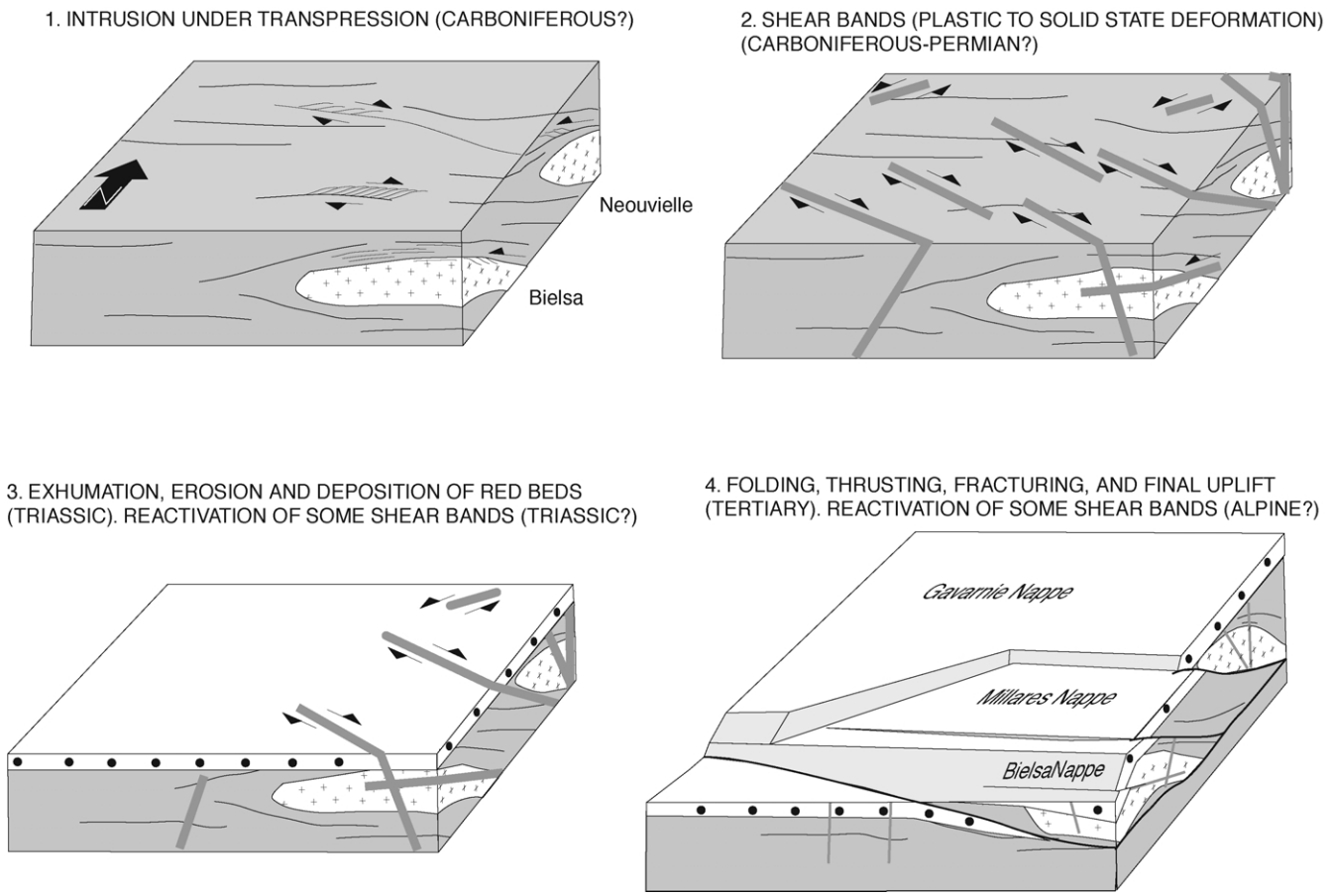

Fig. 12. Block-diagrams showing the evolution proposed for the Bielsa massif from its intrusion during the Carboniferous till its definitive exhumation in Tertiary times. In the first sketch, transpression is indicated by a dextral component in the horizontal plane and a reverse component in the vertical plane.

directly interpreted in the Bielsa granite. Other evidence supporting emplacement under dextral transpression in the Bielsa granite are high temperature solid-state structures in some sites, shear criteria in the country rocks and also dominantly dextral shear bands sealed by unconformable Triassic strata (southern border). Therefore, the intrusion of the Bielsa granite occurred during combined NE–SW flattening and dextral strike-slip movement at least in the later episodes of intrusion, when magma was cooling (Fig. 12). From the P' and T maps (Fig. 10d and e), we infer that the pluton underwent a partition of its deformation in relation to its emplacement, between a strong planar anisotropy along its northern border contrasting with a weak and linear anisotropy along its axis. The occurrence of shear bands and deformation partitioning processes coeval with the emplacement of granites is evidence supporting transpressional conditions (Saint-Blanquat et al., 1998; Vegas et al., 2001).

The Bielsa granite is located in the southernmost part of the Pyrenean Axial Zone, 15 km south of the Neouvielle granite. Considering the displacement of the Palaeozoic nappes during the Tertiary, the whole Axial Zone was 60 km wide before compression (Martínez-Peña and Casas-Sainz, 2003) and the original distance between the Bielsa and the Neouvielle igneous bodies was about 30 km before Tertiary compression. This supports the hypothesis that the Variscan transpression in the Pyrenees was not constrained to a narrow E–W corridor in the northern part of the Axial Zone but was an orogen-scale tectonic regime that involved at least all the present-day outcrop of palaeozoic rocks. During the late stages of granite solidification, deformation was localised along shear bands, consistent with the overall transpressional regime (Fig. 12).

This work demonstrates that some of the shear bands cutting across the Bielsa granite are of clear post-Variscan origin, as pointed out by Soula et al. (1986c), and are associated with alteration of the granitic rock. Given the thickness of the Triassic series and the deformational mechanisms, deformation took place near the surface. The bulk deformation associated with these bands is consistent with NNE–SSW shortening and dominant dextral shear, that is, an overall dextral transpression. In some cases they correspond to reactivated Variscan shear bands. Their most probable origin is related to Late-Variscan deformation during Triassic times, probably related to mineralisations in the Triassic rocks (Yuste, 2000; Yuste et al., 2001). This means that the dextral transpressional regime was not linked

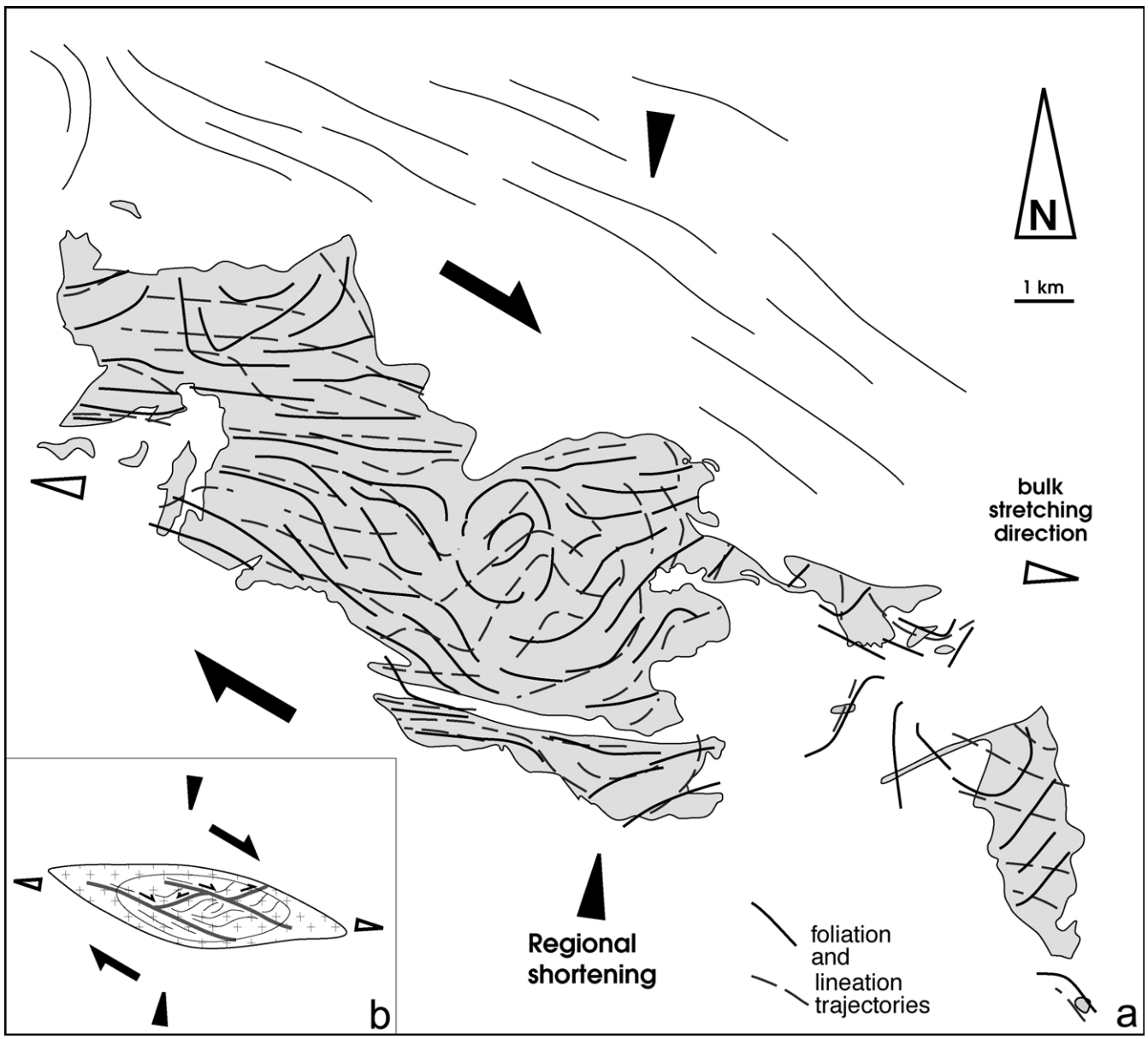

Fig. 13. (a) Proposed model of emplacement and coeval deformation of the Bielsa granite pluton. (b) General sketch of the kinematic context for the model proposed.

to particular depth conditions, but extended through several kilometres (from the emplacement depth of the granite to near-surface conditions) and a considerable time-space (more than 20 m.a.). Some of the shear bands were also reactivated during the Tertiary (Fig. 12), since they were weakness zones liable to localise brittle deformation of the granitic body.

6. Conclusions

This original structural study of the Bielsa granite reveals the existence of dextral shear bands of both Variscan and post-Triassic ages. The age of some bands is demonstrated to be Variscan where they are sealed by Triassic materials (southern border of the pluton). In places where the shear bands rework Triassic sediments, as frequently observed in the eastern part of the pluton, their post-Triassic activity is also demonstrated. However these shear-bands, which cannot be distinguished from the Variscan ones, are likely originally Variscan ones that have been reactivated during post-Triassic times.

The rock-magnetic study evidence that the Bielsa granite is actually not paramagnetic, since the presence of magnetite is evidenced by the thermal demagnetisation of three IRM components and the hysteresis loops.

Anisotropy of magnetic susceptibility (AMS) throughout the Bielsa granite is consistent with field structures and

indicates WNW–ESE striking foliation with variable dip, and subhorizontal WNW–ESE lineation. Foliations and lineations are parallel to the elongation of the massif in map view and to the major structural directions of the country rocks, attributed to the main Variscan phases. The zonation of bulk low-field susceptibility is, in a general way, related to mineral content and indicates a more basic composition at the northeastern and eastern parts of the pluton, where the border facies crops out, and a metamorphic aureole is developed in the country rock. The magnetic anisotropy is at a maximum in the northeastern border where preferred orientation of minerals is very strong. The zonation of shape of the magnetic ellipsoid indicates a partitioning of deformation showing prolate ellipsoids along a central band parallel to the elongation of the massif in map view, and oblate ellipsoids at the borders of the pluton where flattening is more important. Mapping of foliations and lineations of the Bielsa Massif shows a concentric pattern at the central part, suggesting a root zone. Structures within the granitoid body and the country rock allow the interpretation of this intrusion as contemporary to a transpressional setting, syntectonic with the late stages of the Variscan orogeny. According to deformational structures within the granite, this regime probably extended to Late-Variscan times. The Alpine orogeny seems to have imprinted the granite only with brittle faults and reactivation of earlier shear zones.

Acknowledgements

Earlier drafts of this manuscript were greatly improved by helpful comments from J.M. Tubía and G. Gleizes. The authors thank J.L. Bouchez and K. Benn for instructive reviews of the paper. We also thank the University of the Pais Vasco for allowing us to make free use of the KLY-2 susceptibility meter, M. Tricas for the realisation of thin sections, E. Guerrero for technical assistance with the SQUID magnetometer and A. Puzo and M. Gracia for their help with collection of samples. This work forms part of the research projects BTE2002-04168 and BTE2001-0634 (DGES, Spanish Ministry of Education) and UZ00-CIEN-09 (University of Zaragoza).

References

Aranguren, A., Tubía, J.M., Bouchez, J.L., Vigneresse, J.L., 1996. The Guitiriz granite, Variscan belt of northern Spain: extension-controlled emplacement of magma during tectonic escape. Earth and Planetary Science Letters 139, 165–176.

Beck Jr, M., Burmester, R.F., Cembrano, J., Drake, R., Garcia, A., Herve, F., Munizaga, F., 2000. Paleomagnetism of the North Patagonian Batholith, southern Chile; an exercise in shape analysis. Advances in paleomagnetism and tectonics of active margins. Tectonophysics 326 (1–2), 185–202.

Borradaile, G.J., Henry, B., 1997. Tectonic applications of magnetic susceptibility and its anisotropy. Earth-Science Reviews 42 (1–2), 49–93.

Borradaile, G.J., Werner, T., 1994. Magnetic anisotropy of some phyllosilicates. Tectonophysics 235, 223–248.

Bouchez, J.L., 1997. Granite is never isotropic: an introduction to AMS studies of granitic rocks. In: Bouchez, J.L., Hutton, D.H.W., Stephen, W.E. (Eds.), Granite: From Segregation of Melt to Emplacement Fabrics, Kluwer Academic Publishers, pp. 95–112.

Darrozes, J., Moisy, M., Olivier, P., Améglio, L., Bouchez, J.L., 1994. Structure magmatique du granite du Sidobre (Tarn, France): de l'échelle du massif à celle de l'échantillon. Comptes Rendus de l'Académie des Sciences de Paris 318, 243–250.

Day, R., Fuller, M., Schmidt, V.A., 1977. Hysteresis properties of titanomagnetites: grain-size and compositional dependence. Physics of the Earth and Planetary Interiors 13, 260–267.

Déramond, J., Graham, R.H., Hossack, J.R., Baby, P., Crouzet, G., 1985. Nouveau modèle de la chaîne des Pyrénées. Comptes Rendus de l'Académie des Sciences de Paris 301, 1213–1216.

Enrique, P., 1989. Caracterización geoquímica mediante elementos mayores de los granitoides de la vertiente meridional del Pirineo Central. Studia Geologica Salmanticensia 4, 41–60.

Evans, J.P., 1988. Deformation mechanisms in granitic rocks at shallow crustal levels. Journal of Structural Geology 10 (5), 437–443.

Evans, N., Gleizes, G., Leblanc, D., Bouchez, J.L., 1998. Syntectonic emplacement of the Maladeta granite (Pyrenees) deduced from relationships between Hercynian deformation and contact metamorphism. Journal of the Geological Society of London 155, 209–216.

Fisher, R.A., 1953. Dispersion on a sphere. Proceedings of the Real Society of London A217, 295–305.

Frost, B.R., Lindsley, D.H., 1991. Occurrence of iron–titanium oxides in igneous rocks. In: Lindsley, D.H. (Ed.), Oxide Minerals: Petrologic and Magnetic Significance. Reviews in Mineralogy 25, pp. 433–468.

Gleizes, G., Nédélec, A., Bouchez, J.-L., Autran, A., Rochette, P., 1993. Magnetic susceptibility of the Mont Louis–Andorra ilmenite-type granite (Pyrenees): a new tool for the petrographic characterization and regional mapping of zoned granite plutons. Journal of Geophysical Research 98, 4317–4331.

Gleizes, G., Leblanc, D., Bouchez, J.L., 1997. Variscan granites of the Pyrenees revisited: their role as syntectonic markers of the orogen. Terra Nova 9, 37–40.

Gleizes, G., Leblanc, D., Bouchez, J.L., 1998. The main phase of the Hercynian orogeny in the Pyrenees is a dextral transpression. In: Holdsworth, R.E., Strachan, R.A., Dewey, J.F. (Eds.), Continental Transpressional and Transtensional Tectonics. Geological Society, London, Special Publications 135, pp. 267–273.

Gleizes, G., Leblanc, D., Santana, V., Olivier, P., Bouchez, J.L., 1998b. Sigmoidal structures featuring dextral shear during emplacement of the Hercynian granite complex of Cauterets–Panticosa (Pyrenees). Journal of Structural Geology 20, 1229–1245.

Gleizes, G., Leblanc, D., Olivier, P., Bouchez, J.L., 2001. Strain partitioning in a pluton during emplacement in transpressional regime: the example of the Néouvielle granite (Pyrenees). International Journal of Earth Sciences 90, 325–340.

Grégoire, V., Darrozes, J., Gaillot, P., Nédélec, A., 1998. Magnetite grain shape fabric and distribution anisotropy vs rock magnetic fabric: a three-dimensional case study. Journal of Structural Geology 20, 937–944.

Jelinek, V., 1977. The Statistical Theory of Measuring Anisotropy of Magnetic Susceptibility of Rocks and its Application, Geofyzika, Brno, pp. 1–88.

Jelinek, V., 1981. Characterization of the magnetic fabric of rocks. Tectonophysics 79, 63–70.

Jover, O., Rochette, P., Lorand, J.P., Maeder, M., Bouchez, J.L., 1989. Magnetic mineralogy of some granites from the French Massif Central: origin of their low-field susceptibility. Physics of the Earth and Planetary Interiors 55, 79–92.

Launeau, P., 1990. Analyse numérique des images et orientations

préférentielles de forme des agrégats polyphasés: application à l'analyse cinématique des granites. Ph.D. thesis, Université de Toulouse.

Launeau, P., Cruden, A.R., 1998. Magnetic fabric acquisition mechanisms in a syenite: results of a combined anisotropy of magnetic susceptibility and image analysis study. Journal of Geophysical Research 103, 5067–5089.

Launeau, P., Robin, P.Y., 1996. Fabric analysis using the intercept method. Tectonophysics 267, 91–119.

Leblanc, D., Gleizes, G., Lespinasse, P., Olivier, P., Bouchez, J.L., 1994. The Maladeta granite polydiapir, Spanish Pyrenees: a detailed magneto-structural study. Journal of Structural Geology 16, 223–235.

Leblanc, D., Gleizes, G., Roux, L., Bouchez, J.L., 1996. Variscan dextral transpression in the French Pyrenees: new data from the Pic des Trois–Seigneurs granodiorite and its country rocks. Tectonophysics 261, 331–345.

Lowrie, W., 1990. Identification of ferromagnetic minerals in a rock by coercivity and unblocking temperature properties. Geophysical Research Letters 17, 159–162.

Martínez-Peña, B., Casas-Sainz, A., 2003. Cretaceous–Tertiary tectonic inversion at the Cotiella Nappe (Southern Pyrenees, Spain). International Journal of Earth Sciences (Geol. Rundschau), 92, 99–113 (DOI: 10.1007/s002-0283-x).

Mirouse, R., Barrère, P., 1993. Carte Géologique de la France à 1/50000. Vielle-Aure (1083). BRGM.

Muñoz, J.A., 1992. Evolution of a continental collision belt: ECORS–Pyrenees crustal balanced cross-section. In: McClay, K.R., (Ed.), Thrust Tectonics, pp. 235–246. Chapman & Hall, London.

Paquette, J.-L., Gleizes, G., Leblanc, D., Bouchez, J.-L., 1997. Le granite de Bassiès (Pyrénées): un pluton syntectonique d'âge Westphalien. Géochronologie U–Pb sur zircons. Comptes Rendus de l'Académie des Sciences de Paris 324, 387–392.

Pignotta, G.S., Benn, K., 1999. Magnetic fabric of the Barrington Passage pluton, Meguma Terrane, Nova Scotia: a two-stage fabric history of syntectonic emplacement. Tectonophysics 307, 75–92.

Pueyo, E.L., Román-Berdiel, T., Casas-Sainz, A.M., 1995. Determining emplacement mechanisms of granitoids: application of structural and magnetic methods (ASM & IRM zoning). Journal of Czech Geological Society 40 (3), 72.

Ríos-Aragüés, L.M., Lanaja-del-Busto, J.M., Ríos-Mitchell, J.M., Marín-Blanco, F.J., 1982. Mapa Geológico de España E: 1/50000, Hoja de Bielsa (179). IGME.

Roberts, M.P., Pin, C., Clemens, J.D., Paquette, J.-L., 2000. Petrogenesis of mafic to felsic plutonic rock associations: the calc–alkaline Quérigut Complex, French Pyrenees. Journal of Petrology 46 (6), 809–844.

Rochette, P., 1987. Magnetic susceptibility of the rock matrix related to magnetic fabric studies. Journal of Structural Geology 9, 1015–1020.

Romer, R.L., Soler, A., 1995. U–Pb age and lead isotopic characterization of Au-bearing skarn related to the Andorra granite (central Pyrenees, Spain). Mineralium Deposita 30, 374–383.

Saint-Blanquat, M., Tikoff, B., Teyssier, C., Vigneresse, J.L., 1998. Transpressional kinematics and magmatic arcs. In: Holdsworth, R.E., Strachan, R.A., Dewey, J.F. (Eds.), Continental Transpressional and Transtensional Tectonics. Geological Society, London, Special Publications 135, pp. 327–340.

Séguret, M., 1972. Étude tectonique des nappes et séries décollées de la partie centrale du versant sud des Pyrénées. Publications de l'Université des Sciences et Techniques du Languedoc. Série Géologie Structurale.

Soula, J.C., Debat, P., Déramond, J., Pouget, P., 1986a. A dynamic model of the structural evolution of the Hercynian Pyrenees. Tectonophysics 129, 29–51.

Soula, J.C., Debat, P., Déramond, J., Guchereau, J.-Y., Lamouroux, C., Pouget, P., Roux, L., 1986b. Évolution structurale des ensembles métamorphiques, des gneiss et des granitoïdes dans les Pyrénées Centrales. Bulletin de la Société Géologique de France 8 (II, 1), 79–93.

Soula, J.C., Lamouroux, C., Viallard, P., Bessière, P., Debat, P., Ferret, B., 1986c. The mylonite zones in the Pyrenees and their place in the alpine tectonic evolution. Tectonophysics 129, 115–147.

Tikoff, B., Greene, D., 1997. Stretching lineations in transpressional shear zones: an example from the Sierra Nevada Batholith, California. Journal of Structural Geology 19, 29–39.

Vegas, N., Aranguren, A., Tubía, J.M., 2001. Granites built by sheeting in a fault stepover (the Sanabria Massifs, Variscan Orogen, NW Spain). Terra Nova 13, 180–187.

Williams, G.D., 1985. Thrust tectonics in the south central Pyrenees. Journal of Structural Geology 7 (1), 11–18.

Yuste, A., 2000. Mineralizaciones filonianas de F–Pb de Bielsa (Pirineos Aragoneses); papel de los fluidos sintectónicos en su génesis. Tesis Doctoral, Universidad de Zaragoza.

Yuste, A., Subías, I., Fernández-Nieto, 2001. Geochemical and FIP study of three sheared veins from Spanish Central Pyrenees. In: Piestrzynski, A., et al. (Eds.), Mineral Deposits at the Beginning of the 21st Century. Proceedings of the Joint Sixth Biennial SGA-SEG Meeting, Kraków, pp. 497–500. Balkema Publishers, Tokyo.

Zwart, H.J., 1986. The Variscan geology of the Pyrenees. Tectonophysics 129, 9–27.